5-2020

Mitochondrial Deletions and Their Disease-Causing Effects

Austin Bell

Mitochondrial Deletions and Their Disease-Causing Effects

An Honors Thesis submitted in partial fulfillment of the requirements of Honors Studies in Biology

By

Austin Bell

Spring 2020
Biology
J. William Fulbright College of Arts and Sciences
The University of Arkansas

Acknowledgements

There are many people who have helped me throughout my time working on this project and while constructing my thesis. Specifically, I would like to offer my sincere thanks to the following people for the exceptionally positive impact that they have had on me and my project.

I would first like to thank Dr. Shilpa Iyer for giving me the opportunity to work in her research lab and for the volume of work she put in for me as the advisor for my honors thesis project. I would also like to thank Joshua Stabach for all of the time and work he put in with me directly in the lab while working on my project, from teaching me the basics of the lab when I first joined, to showing me what I would need to do when imaging and acquiring data, and finally to helping me with my honors thesis project. Additionally, I thank Ajibola Bakare for the time he spent showing me how to work the different programs used in the lab, the different protocols that he provided for me to help with my project, and for the work he has put in to helping with my honors thesis.

I would next like to thank the University of Arkansas Honors College and the Biology Department within the J. William Fulbright College of Arts and Sciences for the support and opportunity to conduct this research and work on this project. I thank Dr. Shilpa Iyer, Dr. Francis Millett, Dr. Daniel Lessner, and Dr. Kate Chapman for serving on my honors thesis committee. Finally, I would like to thank all of my family and friends who have supported me throughout all of my goals, especially in this project.

Table of Contents

Abstract

The mitochondria perform a plethora of important functions within the cell, with one of the most paramount being ATP production. Deregulation of its function can have dire consequences on cellular functions. Mutations such as deletions within the mitochondrial DNA (mtDNA) can cause disease within the patients affected. These diseases often affect children, causing symptoms such as gradual loss of eyesight and hearing, diabetes, and other problems that lower the quality of life. The mitochondria are also very dynamic organelles that undergo rounds of fission and fusion to keep up with the metabolic needs of cells, necessitating a homeostatic balance between these processes in healthy mitochondria. While advances in technology continue to highlight various novel functions of the mitochondria, our understanding of how various mitochondrial DNA (mtDNA) affects mitochondrial structure and function is still lagging. In this study, we examine the effects of mtDNA deletions on the structure and function of the mitochondria. Using the Mitochondrial Network Analysis tool (MiNA), we were able to identify structural changes in mitochondria of patient fibroblast cell lines with mtDNA deletions. These structural changes correspond to a subsequent decrease in mitochondrial membrane potential (MMP), a measure of mitochondria health. Result from this study suggests a relationship between mitochondrial structural remodeling and function in diseased fibroblast cell lines.

Introduction

The importance of the mitochondria in a cell stretches far beyond only being the "powerhouse of the cell." Although the primary function of synthesizing energy in the form of adenosine triphosphate, known as ATP, within the inner mitochondrial membrane is vital to the

cell; the mitochondria is involved in many other important functions. Mitochondria are important regulators of apoptotic and necrotic cell death, innate immunity, autophagy, redox signaling, and stem cell reprograming, among other such functions (Tilokani et al., 2018). Their crucial nature in many different cellular functions means that mitochondrial structure, including appropriate size, shape, and distribution, are very important for maintaining different tissues' homeostasis. With the advancement of high-resolution microscopy techniques, there has been a growing understanding of mitochondrial dynamics, such as fusion, fission, and autophagy, and their ability to segregate, remove, and dilute damaged mitochondria inside a cell (Eisner et al., 2018).

To help the cell function properly, the mitochondria often moves throughout the cell. This is accomplished in mammalian cells by traveling through the cytoskeleton on polymers of tubulin called microtubules (Ni et al., 2015). The mitochondria are transported to areas with a high energy demand within the cell in order to correctly distribute ATP production and regulate the buffering of Ca^{2+}. The movement of mitochondria also helps support other parts of mitochondrial dynamics such as fusion, fission, and the recycling of the organelle itself (Eisner et al., 2018).

The mitochondria also have their own set of mitochondrial DNA (mtDNA) which consists of 16,569 base pairs organized into a double stranded, circular molecule (Nissanka et al., 2019). The genes that are encoded by this mtDNA are necessary for oxidative phosphorylation in the cell. If deletions occur in the mtDNA, there can be malfunctions in the expression of essential genes, resulting in various mitochondrial disorders. These deletions are thought to possibly be caused by double strand breaks or replication errors, although the exact cause is still unknown (Nissanka et al., 2019). This study focuses two of the most prevalent mitochondrial diseases arising from the deletion of mtDNA, Kearns-Sayre Syndrome and Pearson Syndrome, as a model

for understanding the relationship between mitochondrial structure and function in health and disease.

Patients diagnosed with Kearns-Sayre Syndrome (KSS) have progressive external ophthalmoplegia, which is progressive loss of the ability to move the eyes and eyebrows; pigmentary retinitis, which causes decreased vision at night or in dim light; and an onset of the disease before the age of 20. Other symptoms include deafness and heart blockage which can be fatal (Goldstein & Falk, 2003). These clinical symptoms are a result of the cells carrying dysfunctional mitochondria due to deletions in the mitochondrial genome. In this study, a pediatric KSS patient's fibroblast cells (SBG8) carrying a natural 4.1 kb mtDNA deletion was characterized for defects in the mitochondrial structure and its relationship to mitochondrial function.

Pearson Syndrome (PS) can cause anemia and interfere with the functioning of the pancreas. This can lead to diabetes and even fatality in infants if insulin is not produced at the correct levels (Goldstein & Falk, 2003). In this study, fibroblast cells from two PS patients were used (SBG9 and SBG10). The disease was caused by naturally occurring deletions of 2.5 kb in the SBG9 cell line and 5.4 kb in the SBG10 line. Further studies in the literature have shown that patients suffering from mitochondrial diseases have low energy, measured in the form of reduced base levels of respiration (Nissanka et al., 2019). Both the mitochondrial structure and mitochondrial functioning within the cells of these KSS and PS patients is unknown and has been the focus of this study. We hypothesized that an increase in fragmentation and a decrease in number of branches in the mitochondrial network of the diseased cells leads to a corresponding defect in mitochondrial functions, as measured through Mitochondrial Membrane Potential (MMP) and mitochondrial Reactive Oxygen Species (ROS) production.

For this study, the well-characterized mitochondrial uncoupler FCCP (Carbonyl cyanide 4-(trifluoromethoxy)phenylhydrazone), which is known to disrupt oxidative phosphorylation, was used to understand the connection between mitochondrial shape and its effect on mitochondrial function. FCCP uncouples the oxidation of reducing equivalents (NADH, $FADH_2$) from the phosphorylation of ADP to ATP. FCCP was used to cause cells to simulate a stressed state and induce morphological changes. The control and experimental cell lines were each tested both with and without treatment with FCCP in order to test for a connection between morphological change and bioenergetics within the mitochondria. The results showed differences in mitochondrial structure and membrane potential between the control and diseased cell lines.

Methods

Cell Culturing: All fibroblast cell lines were maintained in culture until passage 8. The cells were all cultured in Minimum Essential Media (MEM; Gibco, U.S.A) supplemented with 10% Fetal Bovine Serum (FBS; Hyclone, U.S.A), and 2mM of L-Glutamine (Gibco, U.S.A). The culture and passaging were done according to the established lab protocols.

Cell Imaging for MiNA: A day prior to experiment, cells were seeded in 35 mm^2 dishes and incubated overnight. On the day of the experiment, culture media was aspirated and washed with dPBS (Dulbecco's Phosphate Buffered Saline). For the FCCP (Carbonyl cyanide 4-(trifluoromethoxy)phenylhydrazone; Sigma, U.S.A) treatment group, FCCP was added to the appropriate dishes at a concentration of 0.7 uM. The dishes were then incubated for 30 minutes and rinsed with basal media. Next, 2 mL of a staining solution with a 150 nM concentration of MitoTracker Red CM-H2Xros (Thermo Fisher Scientific, U.S.A) was added. This was then incubated for another 40 minutes. After this incubation, 2 mL of the Nucblue (Hoechst 33342; Thermo Fisher Scientific, U.S.A) stain were added, and the cells were incubated a final time for

20 minutes. The stain was then aspirated from the dishes, the cells were rinsed with warm PBS, and 2 mL of warm basal MEM was added. Fluorescent and phase contrast images were acquired at 40X magnification for each dish and cell line using EVOS FL microscope. Approximately 9-12 images were taken per dish, with 5 dishes per cell line and treatment group. These images were saved for further analysis.

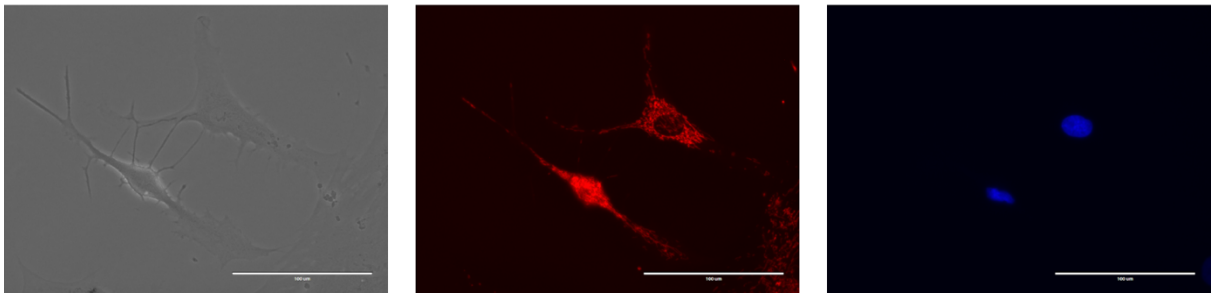

Figure 1: An example of Control cells that were stained and imaged.

Image Analysis: The acquired images were then analyzed using the Mitochondrial Network Analysis (MiNA) plug-in software for ImageJ, which allows for a semi-automated analysis of the mitochondrial networks in the cells (Valente et al., 2017). First, the desired RFP image was opened in ImageJ. Once the image was properly prepared in ImageJ by subtracting the background and adjusting the brightness levels, the image was made into a binary image and then skeletonized. Skeletonized images were opened in Photoshop to isolate individual skeletons, corresponding to an individual cell, as their own image. The isolated individual cellular skeletons were re-opened in ImageJ and the MiNA plugin was employed to generate data on different morphological components of the mitochondria. The surface area of each cell was also found using Image J. Each morphological component derived from MiNA was divided by the specific cell surface area to normalize for differences in cell size. The mean and standard deviation (S.D.) were calculated for each parameter. Data which was found to be two standard deviations away from the mean was excluded as an outlier.

Figure 2: An example of two BJ cells separated into individual skeletonized images.

Mitochondrial ROS and Mitochondrial Membrane Potential: Cells were cultured to the appropriate passage (P8) and confluency (80%). On the day of the experiment, cells were enzymatically detached and divided into their respective treatment groups. The treatment groups for the mitochondrial membrane potential (MMP) experiments were arranged as follows: Non-Treated, TMRE (Tetramethylrhodamine, ethyl ester; Abcam, U.S.A) only, TMRE + FCCP, and TMRE + Oligomycin (Sigma, U.S.A). The final well concentrations of 50 nM TMRE, 20 µM FCCP, and 5 µM Oligomycin were applied to the respective cells. The treatment groups for mitochondrial Reactive Oxygen Species (mitoROS) experiments were arranged as follows: Non-treated, and MitoSox (Thermo Fisher Scientific, U.S.A) only. Final well concentrations of 3µM MitoSox were applied to the respective cells. In the MMP experiments, the cells were treated with the mitochondrial inhibitors (FCCP and Oligomycin) ten minutes prior to treatment with TMRE. This was followed by incubation for 25 minutes. At the end of the incubation period, cells were centrifuged and resuspended in dPBS to get rid of excess stain. The cells were centrifuged a second time and resuspended for flow cytometry analysis. Cells were washed twice with dPBS, centrifuged, resuspended in phenol-Red free MEM, and transferred to an Accuri C6 Flow cytometer for data acquisition (10,000 events were recorded for each well). Flow cytometry data was analyzed using FlowJo_V10 software. The non-treated group was used to gate for live cells and positive cell populations. The geometric mean, a measure of mean

fluorescence intensity, was determined. This value was multiplied by the counts for TMRE/MitoSox positive populations to normalize the data. The data was further analyzed using FlowJo_V10.

Statistical Analysis: All statistics were performed, and graphs made, using GraphPad Prism 8. A one-way ANOVA with post-hoc Tukey was performed with an alpha value of 0.05 to determine statistical significance.

Results

Mitochondrial morphology is perturbed in fibroblast cell lines with mtDNA deletions: Owing to the large-scale deletions in our diseased cell lines, we hypothesized that relative to control cell lines, the diseased fibroblast cell lines will exhibit varied mitochondrial morphology indicative of a diseased state. Furthermore, we introduced FCCP, a potent mitochondrial uncoupler, to mimic metabolic stress. Our results show that the number of individuals was found to be 16% and 12% higher in SBG8 and SBG10 respectively relative to control cell line in the no treatment group (Fig. 4a). While SBG9 showed a slight increase of 2%, this is not statistically significant. Treatment with FCCP did not significantly alter the number of individual mitochondria in the diseased cell lines relative to control. SBG10 had a 17% and 10% increase in number of networks (Fig. 4c) relative to control in the no treatment and FCCP-treatment groups respectively. There was a 35% and 43% decrease in mean branch length (Fig. 4b) for SBG8 compared to healthy control in the no treatment and FCCP treatment groups respectively. The number of networks was not significantly different between the control and diseased cell lines in the no treatment group, however, SBG8 is significantly lower than control in the FCCP treatment (Fig. 4d).

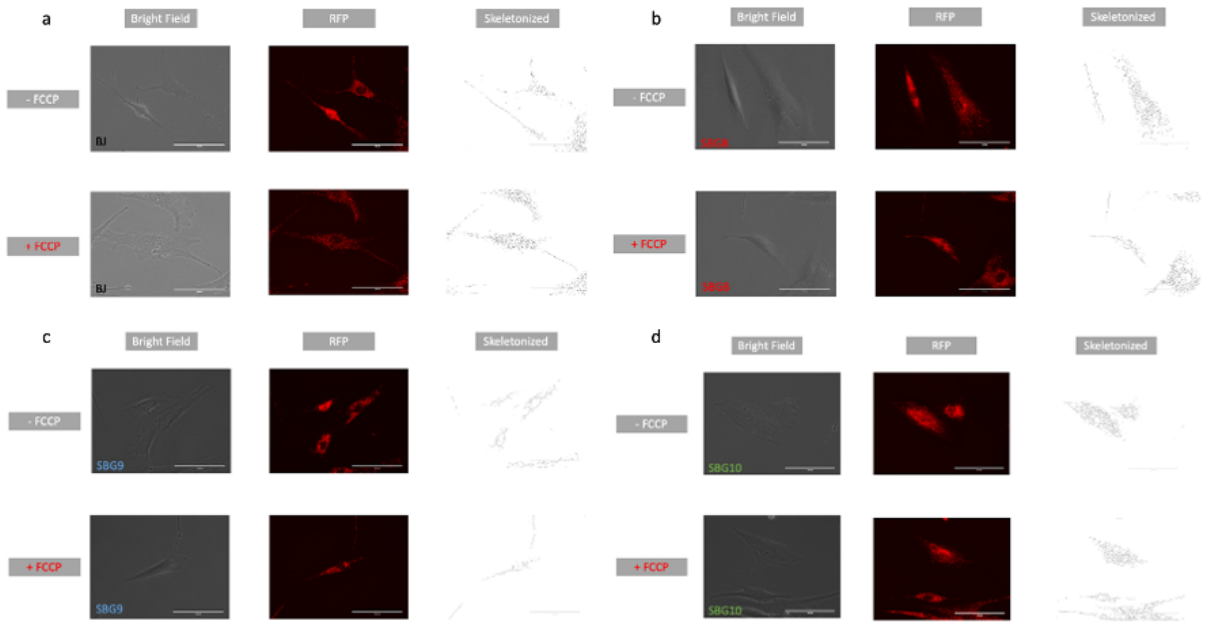

Figure 3: Representative images of different cell lines imaged with and without FCCP. a) Control cell line with and without FCCP b) SBG8 cell line with and without FCCP c) SBG9 cell line with and without FCCP d) SBG10 cell line with and without FCCP.

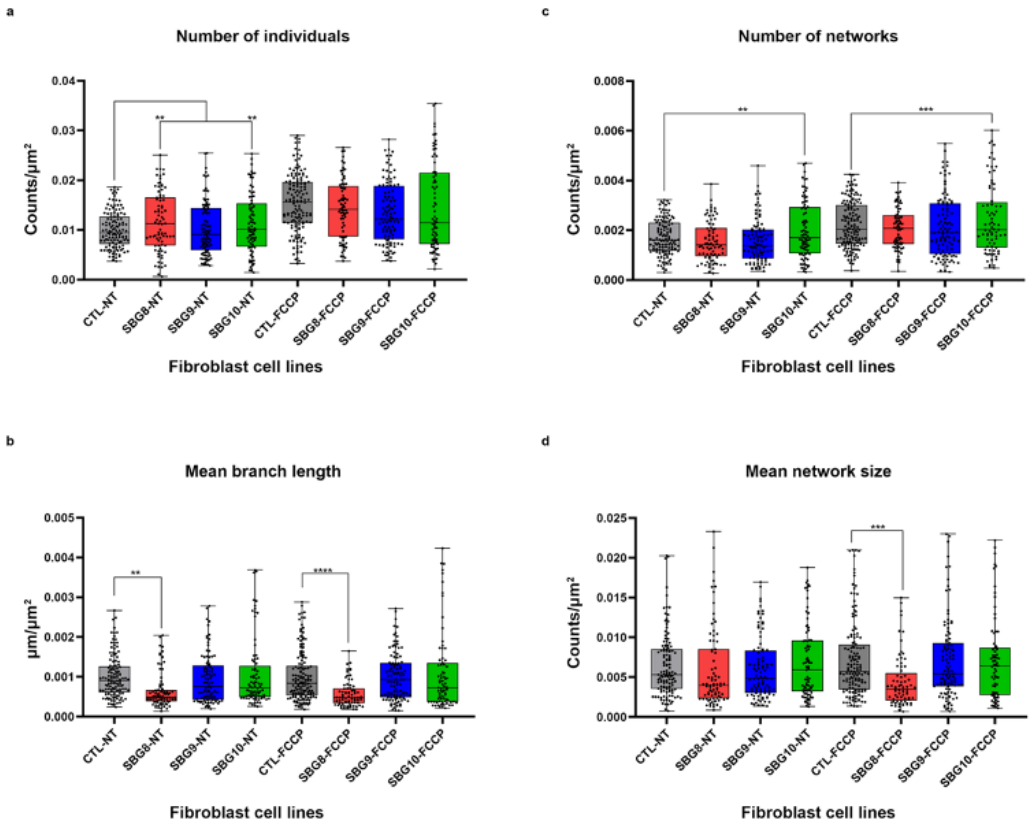

Figure 4: Diseased cell lines show differing morphological traits as compared to the control cell line. a) The number of individual fragments found in the mitochondria for control (CTL) and

diseased (SBG8, 9, and 10) cell lines with (FCCP) and without (NT) treatment b) The average length of each branch of a network in the mitochondria for (CTL) and diseased (SBG8, 9, and 10) cell lines with (FCCP) and without (NT) treatment c) The number of networks of at least two combined individuals in the mitochondria for (CTL) and diseased (SBG8, 9, and 10) cell lines with (FCCP) and without (NT) treatment d) The average number of branches making up the networks in the mitochondria for (CTL) and diseased (SBG8, 9, and 10) cell lines with (FCCP) and without (NT) treatment. *p<0.5, **p<0.1, ***p<0.01, ****p<0.001

Mitochondrial Membrane Potential (MMP) is lower in cell lines with mtDNA deletions: In an effort to understand the relationship between mitochondrial structure and function, we assessed the mitochondrial membrane potential of diseased and healthy fibroblast cell lines. TMRE was used to stain the cells, and two potent mitochondrial inhibitors, FCCP and Oligomycin were used to depolarize and hyperpolarize the mitochondria respectively. Our result showed a 71%-99% decrease in MMP (Fig. 5d) in the diseased fibroblast cell lines relative to the healthy control. When treated with FCCP and Oligomycin, although each cell line responded appropriately to the drug treatments (i.e depolarization and hyperpolarization), the diseased cell lines still showed a trend towards lower MMP (Fig 5e-f).

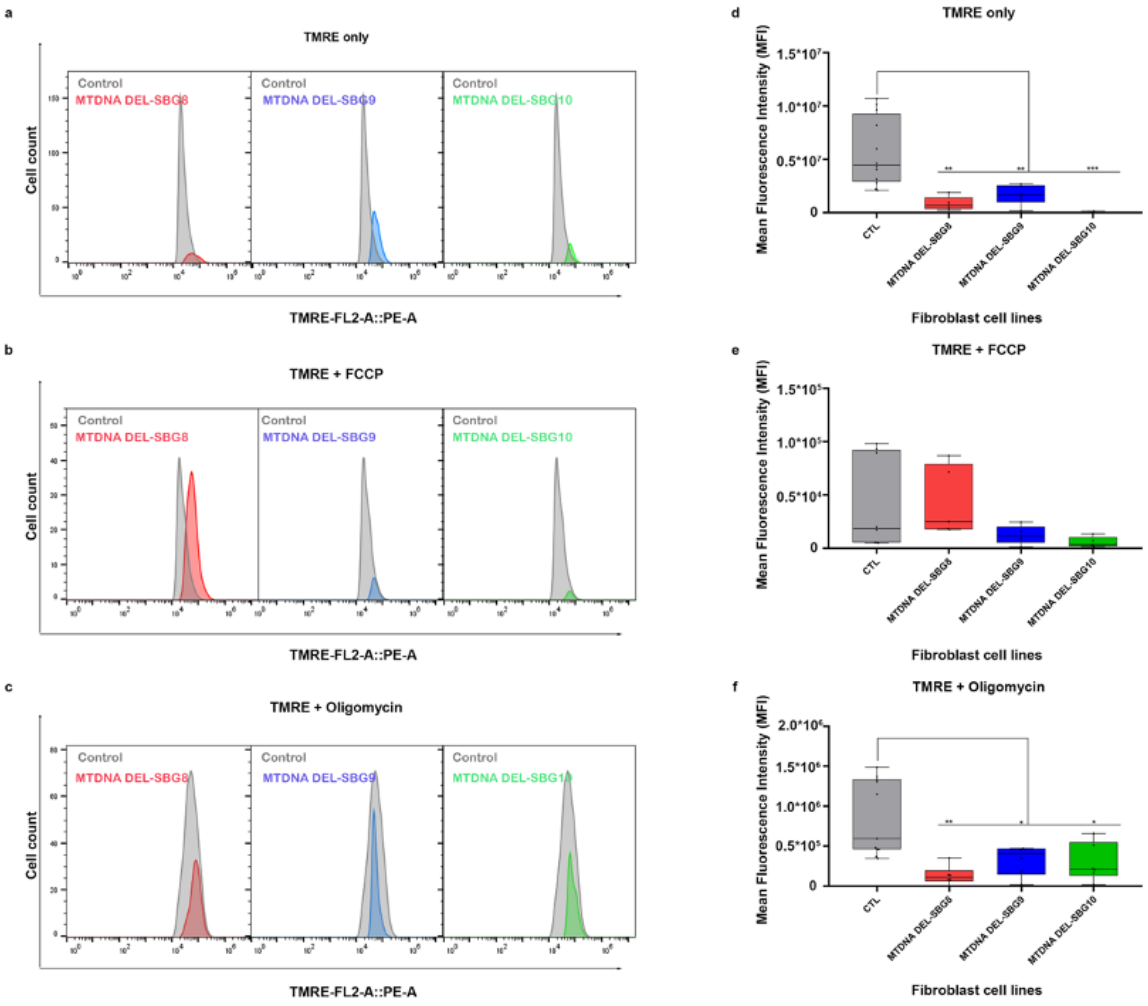

Figure 5: MMP results from flow cytometry show a difference between control and diseased cell lines. a) The number of cells showing different levels of fluorescence with TMRE treatment b) The number of cells showing different levels of fluorescence with TMRE and FCCP treatment c) The number of cells showing different levels of fluorescence with TMRE and Oligomycin treatment d) Comparison of the mean fluorescent intensity of the control (CTL) BJ cell line and the diseased SBG8, 9, and 10 lines when treated with TMRE e) Comparison of the mean fluorescent intensity of the control (CTL) BJ cell line and the diseased SBG8, 9, and 10 lines when treated with TMRE and FCCP f) Comparison of the mean fluorescent intensity of the control (CTL) BJ cell line and the diseased SBG8, 9, and 10 lines when treated with TMRE and Oligomycin. *p<0.5, **p<0.1, ***p<0.01

Mitochondrial ROS production was not affected in mutant cell lines: Finally, ROS production was measured in diseased and control fibroblast cell lines. The MitoSox stain was used to determine if there is a change in reactive oxygen species production in the cell lines with

mtDNA deletions. While there were no statistically significant differences found between the control cell line and any of the diseased cell lines, there is a trend towards lower ROS production (Fig. 6) in most of the diseased cell lines.

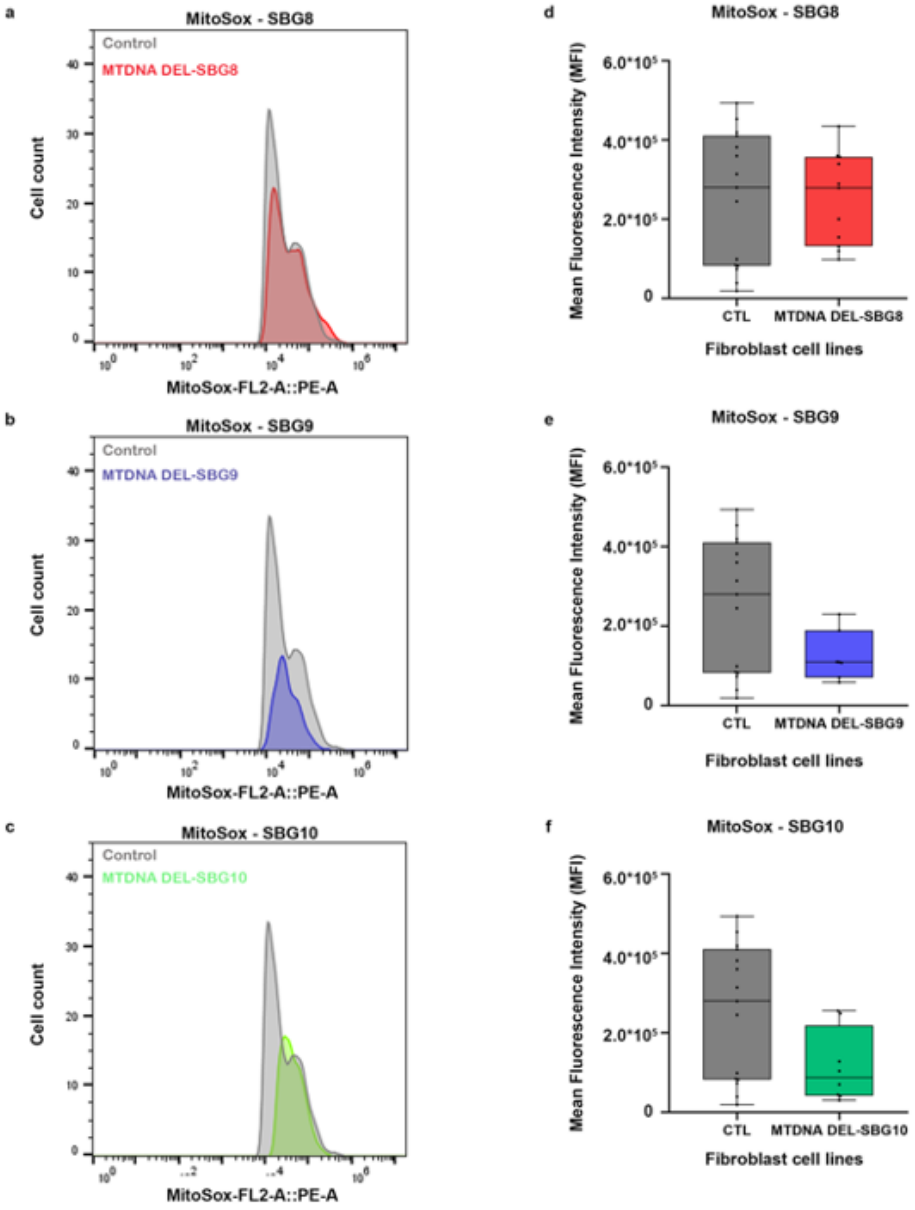

Figure 6: No significant difference was found in the ROS production of control and diseased cell lines. a) The number of SBG8 cells showing different levels of fluorescence with MitoSox treatment b) The number of SBG9 cells showing different levels of fluorescence with MitoSox treatment c) The number of SBG 10 cells showing different levels of fluorescence with

MitoSox treatment d) Comparison of the mean fluorescent intensity of the control (CTL) BJ cell line and the diseased SBG8 cell line e) Comparison of the mean fluorescent intensity of the control (CTL) BJ cell line and the diseased SBG9 cell line f) Comparison of the mean fluorescent intensity of the control (CTL) BJ cell line and the diseased SBG10 cell line.

Discussion

When looking at the data obtained from MiNA analysis (Fig. 4), the SBG8 and SBG10 cell lines have a higher number of individuals than the control cell line. This is consistent with what would be expected from the cells with KSS and PS. The mitochondrial deletions present in these mutations cause increased fragmentation, leading to more individuals. There was no significant difference in number of individuals once FCCP was added, as the FCCP causes distress and increases fragmentation within all the cell lines, consistent with literature findings of mitochondrial remodeling during stress (Goyal et al., 2007). The smaller branch length in the SBG8 cell line as compared to the control cell line with no treatment is also consistent with what would be expected, as the increase in fragmentation would cause the average branch length to decrease. FCCP treatment induced a further decrease in mean branch length in SBG8, suggesting further fragmentation in this cell line relative to control. This could suggest that addition of stress in patients with KSS could potentially exacerbate disease progression. The number of networks was higher for SBG10 than it was for the control in both the no treatment and FCCP treatment groups, this observation is consistent with what is expected, as mitochondria fragmentation would cause more, and smaller, networks. Additionally, the mean network size is smaller in the SBG8 group relative to the control when treated with FCCP. While this was not observed in the no treatment group, it is consistent with predictions for this cell line, as fragmentation will result in a decrease in the size of a network. Altogether, the MiNA results provide evidence for changes in the mitochondrial morphology of cell lines with mtDNA deletions. The MiNA plugin used in these studies has some limitations (Valente et al., 2017) making it difficult to fully comprehend

the various morphological changes associated with a disease state. Future studies that enhance this plugin will provide better analytical power to help delineate the various mitochondrial morphologies in health and disease.

When looking at the flow cytometry data for MMP, the control cells showing more fluorescence than the diseased cells is consistent with what was expected, as this indicative of a higher and healthy MMP (Fig. 5). The MMP is important for keeping the gradient required for ATP production, this is achieved by the various oxidative phosphorylation enzymes. All of the diseased cell lines used in this study have deletions that affect core components of the oxidative phosphorylation enzymes, it is therefore expected that MMP will be affected negatively. The mitochondrial inhibitors FCCP and Oligomycin, which were used to depolarize and hyperpolarize the mitochondria, further highlight defect to the MMP in the diseased cell lines.

Finally, when looking at the mitochondrial ROS (Fig. 6), the fact that there was not any difference indicated was not what would be expected, as the distress that the disease causes the cells would be expected to increase the amount of reactive oxygen species in the diseased cell lines. However, the results of this test did show that there was no effect on mitochondrial ROS production in the diseased cell lines. ROS production is important as it serves as a useful messenger for cellular health (Zorov et al., 2014). Having a relatively lower ROS than predicted could suggest a compensatory mechanism by the diseased cell lines. Future experiments will need to study expression levels of antioxidant and ROS scavengers to clarify how expression levels of these enzymes are different in cells with mtDNA deletion. Taken together, this study suggests a strong relationship between mitochondrial structure and function as it relates to deletions in mtDNA. Future experiments will need to be performed to identify the specific genes

that regulate this observed relationship. Furthermore, bioenergetic assays will help strengthen the relationship between structure and mitochondrial functions in mitochondrial disorders.

References

Eisner, V., Picard, M., & Hajnóczky, G. (2018). Mitochondrial dynamics in adaptive and maladaptive cellular stress responses. *Nature Cell Biology*, *20*(7), 755–765. https://doi.org/10.1038/s41556-018-0133-0

Goldstein, A., & Falk, M. J. (2003). Mitochondrial DNA Deletion Syndromes. *GeneReviews®*. http://www.ncbi.nlm.nih.gov/pubmed/20301382

Goyal, G., Fell, B., Sarin, A., Youle, R. J., & Sriram, V. (2007). Role of Mitochondrial Remodeling in Programmed Cell Death in Drosophila melanogaster. *Developmental Cell*, *12*(5), 807–816. https://doi.org/10.1016/j.devcel.2007.02.002

Ni, H. M., Williams, J. A., & Ding, W. X. (2015). Mitochondrial dynamics and mitochondrial quality control. *Redox Biology*, *4*, 6–13. https://doi.org/10.1016/j.redox.2014.11.006

Nissanka, N., Minczuk, M., & Moraes, C. T. (2019). Mechanisms of Mitochondrial DNA Deletion Formation. *Trends in Genetics*, *35*(3), 235–244. https://doi.org/10.1016/j.tig.2019.01.001

Tilokani, L., Nagashima, S., Paupe, V., & Prudent, J. (2018). Mitochondrial dynamics: overview of molecular mechanisms. *Essays In Biochemistry*, *62*(3), 341–360. https://doi.org/10.1042/ebc20170104

Valente, A. J., Maddalena, L. A., Robb, E. L., Moradi, F., & Stuart, J. A. (2017). A simple ImageJ macro tool for analyzing mitochondrial network morphology in mammalian cell culture. *Acta Histochemica*, *119*(3), 315–326. https://doi.org/10.1016/j.acthis.2017.03.001

Zorov, D. B., Juhaszova, M., & Sollott, S. J. (2014). Mitochondrial reactive oxygen species (ROS) and ROS-induced ROS release. *Physiological Reviews*, *94*(3), 909–950. https://doi.org/10.1152/physrev.00026.2013